Tetrahedron 66 (2010) 9655–9658

Contents lists available at ScienceDirect

Tetrahedron

journal homepage: www.elsevier.com/locate/tet

A highly selective turn-on fluorescent chemosensor for copper(II) ion

Shu-Pao Wu *, Tzu-Hao Wang, Shi-Rong Liu

Department of Applied Chemistry, National Chiao Tung University, Hsinchu, Taiwan 300, Republic of China

ARTICLE INFO

Article history:
Received 2 September 2010
Received in revised form 20 October 2010
Accepted 20 October 2010
Available online 26 October 2010

Keywords:
Cu(II)
Fluorescent chemosensor
Pyrene
Diaminomaleonitrile

ABSTRACT

A new pyrene derivative (**1**) containing a diaminomaleonitrile moiety exhibits high selectivity for Cu^{2+} detection. Significant fluorescence enhancement was observed with chemosensor **1** in the presence of Cu^{2+}. However, the metal ions Ag^{+}, Ca^{2+}, Cd^{2+}, Co^{2+}, Fe^{2+}, Fe^{3+}, Hg^{2+}, Mg^{2+}, Mn^{2+}, Ni^{2+}, Pb^{2+}, and Zn^{2+} produced only minor changes in fluorescence values for the system. The apparent association constant (K_a) of Cu^{2+} binding in chemosensor **1** was found to be 5.55×10^3 M^{-1}. The maximum fluorescence enhancement caused by Cu^{2+} binding in chemosensor **1** was observed over the pH range 5–7.5.

1. Introduction

Copper, after iron, and zinc, is the third most abundant essential transition metal ion in the human body and plays important roles in various biological processes.[1,2] Many proteins contain copper ions as part of a catalytic center. Free copper ions in a live cell catalyze the formation of reactive oxygen species (ROS) that can damage lipids, nucleic acids, and proteins. Research has connected the cellular toxicity of copper ions with serious diseases including Alzheimer's disease,[3] Indian childhood cirrhosis (ICC),[4] prion disease,[5] and Menkes and Wilson diseases.[6,7] Due to its extensive applications, the copper ion is also a significant metal pollutant. The limit of copper in drinking water set by the US Environmental Protection Agency (EPA) is 1.3 ppm (~20 μM).

Numerous methods for the detection of copper ions in a sample have been proposed, including atomic absorption spectrometry,[8] inductively coupled plasma mass spectroscopy (ICPMS),[9] inductively coupled plasma-atomic emission spectrometry (ICP-AES),[10] and voltammetry.[11] Most of these methods cannot be used for assays because they entail the destruction of the sample. Consequently, more attention is being focused on the development of fluorescent chemosensors for the detection of Cu^{2+} ions.[12] Because Cu^{2+} is known as a fluorescence quencher, most fluorescent chemosensors detect Cu^{2+} through a fluorescence quenching process that undergoes an energy or charge transfer mechanism.[12n] Due to their sensitivity, fluorescent chemosensors detecting metal ions using fluorescence enhancement are more easily monitored than those using fluorescence quenching. This paper reports on a newly designed pyrene-based fluorescent enhancement chemosensor for Cu^{2+} based on the photoinduced electron transfer (PET) mechanism. Binding Cu^{2+} to the chemosensor blocks the PET mechanism and greatly enhances the fluorescence of pyrene.

In this study, a pyrene-based fluorescent chemosensor was designed for metal ion detection. Two parts make up chemosensor **1**: a pyrene moiety as a reporter, and diaminomaleonitrile as a chelator for the metal ion (Scheme 1). Chemosensor **1** exhibits weak fluorescence due to fluorescence quenching by photoinduced electron transfer from the lone pair of electrons on the nitrogen atom to pyrene. Binding metal ions to the chemosensor blocks the PET mechanism and results in great fluorescence enhancement of pyrene. The metal ions Ag^{+}, Ca^{2+}, Cd^{2+}, Co^{2+}, Cu^{2+}, Fe^{2+}, Fe^{3+}, Hg^{2+}, Mg^{2+}, Mn^{2+}, Ni^{2+}, Pb^{2+}, and Zn^{2+} were tested for metal ion binding selectivity with chemosensor **1**, but Cu^{2+} was the only ion that caused a visible color change (from yellow to colorless) and a blue emission upon binding with chemosensor **1**.

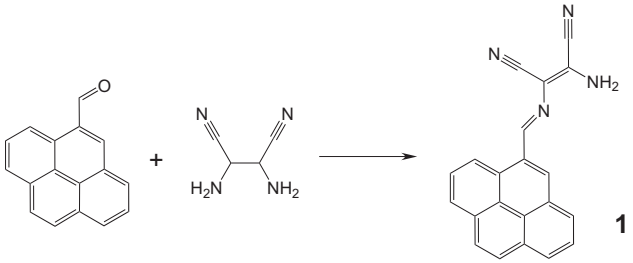

Scheme 1. Synthesis of chemosensor **1**.

* Corresponding author. Tel.: +886 3 5712121x56506; fax: +886 3 5723764; e-mail address: spwu@mail.nctu.edu.tw (S.-P. Wu).

0040-4020/$ – see front matter © 2010 Elsevier Ltd. All rights reserved.
doi:10.1016/j.tet.2010.10.054

2. Results and discussion

2.1. Synthesis

Chemosensor **1** was synthesized through the reaction of diaminomaleonitrile and 1-pyrenealdehyde to form an imine bond between diaminomaleonitrile and pyrene (Scheme 1). Chemosensor **1** is yellow and has an absorption band centered at 421 nm, which is an 86-nm red shift from the typical absorption band of pyrene, 335 nm.[13] Compared to the structure of pyrene, chemosensor **1** has longer conjugated double bonds and its two nitrile groups effectively withdraw electrons. These reasons account for the longer UV–vis absorption wavelength for chemosensor **1** than for pyrene. In addition, chemosensor **1** exhibits weak fluorescence (Φ=0.0045) compared to pyrene (Φ=0.6–0.9).[14] This is due to fluorescence quenching by photoinduced electron transfer from the lone pair of electrons on the nitrogen atom to pyrene.

2.2. Cation-sensing properties

The sensing ability of chemosensor **1** was tested by mixing it with the metal ions Ag^{+}, Ca^{2+}, Cd^{2+}, Co^{2+}, Cu^{2+}, Fe^{2+}, Fe^{3+}, Hg^{2+}, Mg^{2+}, Mn^{2+}, Ni^{2+}, Pb^{2+}, and Zn^{2+}. Cu^{2+} was the only ion that caused a visible color change (from yellow to colorless) and a blue emission from chemosensor **1** (Fig. 1). During Cu^{2+} titration with chemosensor **1**, the absorbance at 420 nm decreased and a new band centered at 355 nm was formed (Fig. 2). The color change from yellow to colorless clearly revealed this 65-nm blue shift. The new band centered at 355 nm is close to the absorption band of pyrene, 335 nm. This indicated that Cu^{2+} binding with chemosensor **1** blocked the electron withdrawing ability of the two-nitrile groups and resulted in a shorter absorption wavelength.

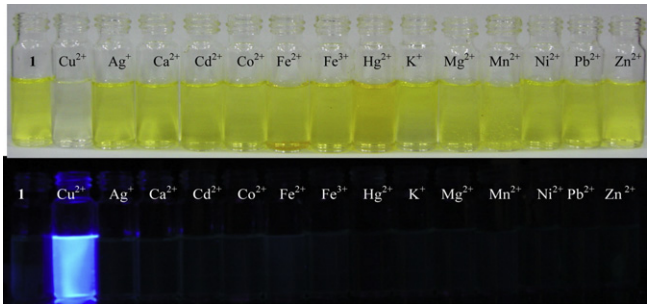

Fig. 1. Color (top) and fluorescence (bottom) changes of chemosensor **1** (25 μM) upon addition of various metal ions (100 μM) in acetonitrile–water (v/v=1:1, 10 mM HEPES, pH=7.0) solutions.

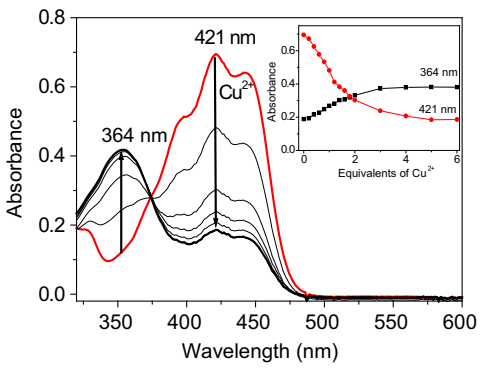

Fig. 2. Absorption changes of chemosensor **1** (25 μM) in the presence of various equivalents of Cu^{2+} in acetonitrile–water (v/v=1:1, 10 mM HEPES, pH=7.0) solutions.

To further evaluate the selectivity of chemosensor **1** toward various metal ions, the fluorescence spectra of chemosensor **1** were taken in the presence of several transition metal ions. However, Cu^{2+} was the only metal ion that caused a significant blue emission (Fig. 1). During Cu^{2+} titration with chemosensor **1**, a new emission band centered at 417 nm formed (Fig. 3). After adding 4 equiv of Cu^{2+}, the emission intensity reached a maximum. The quantum yield of the emission band was 0.59, which is 131-fold that of chemosensor **1** at 0.0045. The emission band and quantum yield of chemosensor **1** are similar to the monomer of pyrene, which has a quantum yield of 0.6–0.9.[10] These observations indicate that Cu^{2+} is the only metal ion that readily binds with chemosensor **1**, causing significant fluorescence enhancement and permitting highly selective detection of Cu^{2+}.

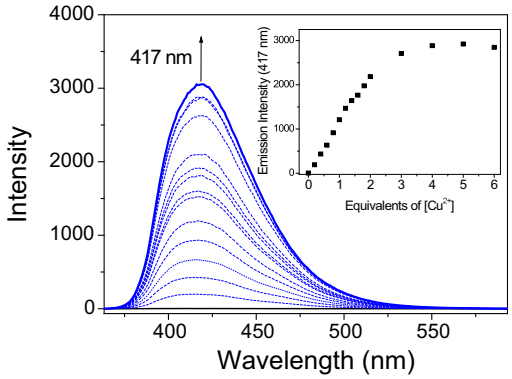

Fig. 3. Fluorescence response of chemosensor **1** (25 μM) to various equivalents of Cu^{2+} in acetonitrile–water (v/v=1:1, 10 mM HEPES, pH=7.0) solutions. The excitation wavelength is 350 nm.

To study the influence of other metal ions on Cu^{2+} binding with chemosensor **1**, this research performed competitive experiments with other metal ions (200 μM) in the presence of Cu^{2+} (100 μM) (Fig. 4). Fluorescence enhancement caused by the mixture of Cu^{2+} with most metal ions was similar to that caused by Cu^{2+} alone. Smaller fluorescence enhancement was observed only when Cu^{2+} was mixed with Fe^{2+} or Fe^{3+} indicating that Fe^{2+} and Fe^{3+} compete with Cu^{2+} for binding with chemosensor **1**. None of the other metal ions was found to interfere with the binding of chemosensor **1** with Cu^{2+}.

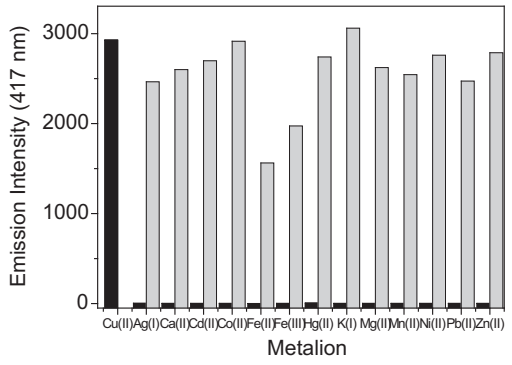

Fig. 4. Fluorescence response of chemosensor **1** (25 μM) to Cu^{2+} (100 μM) or 200 μM of other metal ions (the black bar portion) and to the mixture of other metal ions (200 μM) with 100 μM of Cu^{2+} (the gray bar portion) in acetonitrile–water (v/v=1:1, 10 mM HEPES, pH=7.0) solutions.

In order to understand the binding stoichiometry of **1**–Cu^{2+} complexes, Job plot experiments were carried out. In Fig. 5, the emission intensity at 417 nm is plotted against molar fraction of chemosensor **1** under a constant total concentration. Maximum emission intensity was reached when the molar fraction was 0.5. These results indicate a 1:1 ratio for **1**–Cu^{2+} complexes, in which one Cu^{2+} ion was bound with one chemosensor **1**. The association constant K_a was evaluated graphically by plotting $1/\Delta F$ against $1/[Cu^{2+}]$ (Fig. 6). The data was linearly fit according to the Benesi–Hilderbrand equation and the K_a value was obtained from the slope and intercept of the line. The apparent association constant (K_a) of Cu^{2+} binding in chemosensor **1** was found to be 5.55×10^3 M^{-1}.

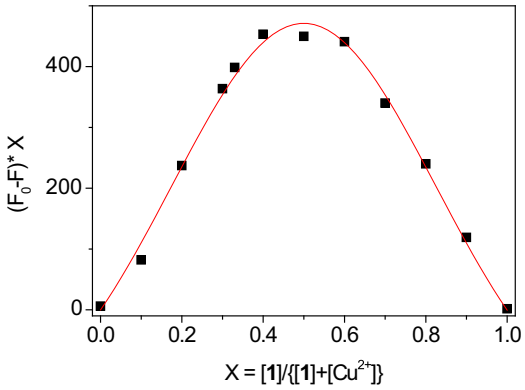

Fig. 5. Job plot of the Cu^{2+}–1 complexes in an acetonitrile–water (v/v=1:1, 10 mM HEPES, pH=7.0) solution. The monitored wavelength is 417 nm.

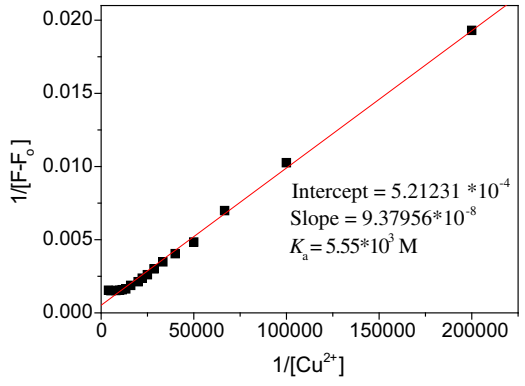

Fig. 6. Benesi–Hildebrand plot of the Cu^{2+}–1 complexes in acetonitrile–water (v/v=1:1, 10 mM HEPES, pH=7.0) solutions.

To gain a clearer understanding of the structure of **1**–Cu^{2+} complexes, ^1H NMR and Infrared (IR) spectroscopy were employed. Cu^{2+} is a paramagnetic ion and can affect the proton signals that are close to Cu^{2+} binding site. In the ^1H NMR spectra of chemosensor **1**, the proton (NH) signal at 6.4 ppm almost completely disappeared upon the addition of Cu^{2+} (Fig. S5 in the supplementary data). Other peaks remained unchanged. These observations indicated the binding of Cu^{2+} with an amine group. The IR spectra were primarily characterized by bands in the double-bond and triple-bond regions. Two bands, 1628 cm^{-1} and 1598 cm^{-1}, were associated with double-bond (C=C and C=N) absorption in chemosensor **1**; two bands, 2232 cm^{-1} and 2204 cm^{-1}, were associated with triple-bond (C≡N) absorptions (Fig. S6 in the supplementary data). Binding of Cu^{2+} with chemosensor **1** resulted in a new broad band at 1646 cm^{-1} in the double-bond absorption region; the band at 1598 cm^{-1} remained unchanged. This was due to Cu^{2+}-induced deprotonation of the amine group in chemosensor **1** during Cu^{2+} binding.[15] Cu^{2+}-induced deprotonation of the amine group formed a charge-delocalized species in the five-member chelating ring. This accounts for the formation of a new broad band at 1646 cm^{-1} upon Cu^{2+} binding. In the triple-bond absorption region, two other bands at 2232 cm^{-1} and 2204 cm^{-1} decreased and a new band at 2154 cm^{-1} was observed upon addition of Cu^{2+}. This indicated that the binding of Cu^{2+} with two amine nitrogens in chemosensor **1** affected the electron withdrawing ability of the two-nitrile groups and resulted in a shorter wavenumber. According to the result of Job plot, the binding ratio for **1**-Cu^{2+} complexes was 1:1, in which one Cu^{2+} ion was bound with one chemosensor **1**. Cu^{2+} was bound to two nitrogens (Fig. 7).

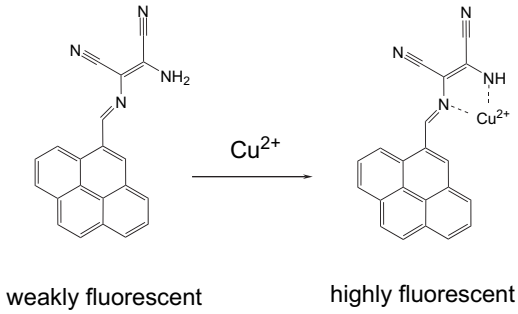

Fig. 7. A proposed 1:1 complex formed between 1 and Cu^{2+}.

The study performed pH titration of chemosensor **1** to investigate a suitable pH range for Cu^{2+} sensing. As depicted in Fig. 8, the emission intensities of metal-free chemosensor **1** were very low. After mixing chemosensor **1** with Cu^{2+}, the emission intensity at 417 nm suddenly increased at pH 5.0 and reached a maximum in the pH range of 5.5–7.5. When pH exceeded higher than 8.5, the emission intensity dropped sharply to zero. This indicates poor stability of the **1**–Cu^{2+} complexes at high pH. For pH <5, the emission intensity is very low due to the protonation of the amine groups that prevents the formation of **1**-Cu^{2+} complexes.

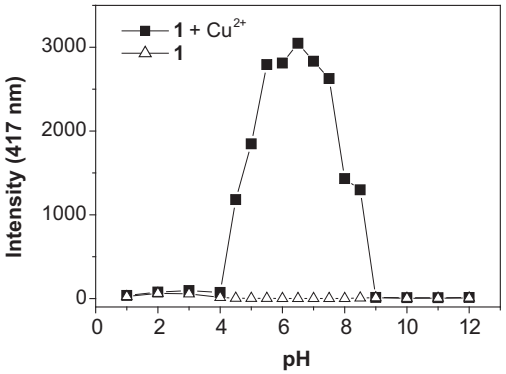

Fig. 8. Fluorescence intensity (417 nm) of free chemosensor **1** (25 μM) (△) and after addition of Cu^{2+} (100 μM) (■) in an acetonitrile–water (v/v=1/1, 10 mM buffer) solution as a function of different pH values. The excitation wavelength was 350 nm.

3. Conclusions

In conclusion, this study developed a pyrene-based fluorescent chemosensor for Cu^{2+} sensing. The experiment synthesized chemosensor **1** from the reaction of diaminomaleonitrile and 1-pyrenealdehyde to form an imine bond between diaminomaleonitrile and pyrene. We observed significant fluorescence enhancement with chemosensor **1** in the presence of

Cu^{2+}. However, adding Ag^{+}, Ca^{2+}, Cd^{2+}, Co^{2+}, Fe^{2+}, Fe^{3+}, Hg^{2+}, Mg^{2+}, Mn^{2+}, Ni^{2+}, Pb^{2+}, or Zn^{2+} to the chemosensor solution caused only minimal change in fluorescence emission. The optimal pH range for Cu^{2+} detection by chemosensor **1** is 5–7.5. This pyrene-based Cu^{2+} chemosensor provides an effective means of Cu^{2+} sensing.

4. Experimental section

4.1. Materials and instrumentations

All solvents and reagents were obtained from commercial sources and used as received without further purification. UV–vis spectra were recorded on an Agilent 8453 UV–vis spectrometer. IR data were obtained on Bomem DA8.3 Fourier-Transform Infrared Spectrometer. NMR spectra were obtained on a Bruker DRX-300 NMR spectrometer.

4.2. Synthesis of 2-((pyren-1-yl)methyleneamino)-3-amino maleonitrile (chemosensor 1)

The reaction mixture containing 1-pyrenecarboxaldehyde (0.230 g, 1.0 mmol) and 1,2-diaminomaleonitrile (1.5 mmol) in acetonitrile was heated, and stirred for 12 h. Color was changed from colorless to yellow. Thereafter, the solvent was evaporated under reduced pressure, and the crude product was purified by column chromatography (ethyl acetate: hexane=2:1) to give **1** as a yellow solid. Yield: 60%; mp: 248–249°C. EI-Mass *m*/*z* (%), 320 (100%), 266(19%), 227(22%); HRMS(EI): $C_{21}H_{12}N_4$ calcd, 320.1062; found, 320.1057. ^{1}H NMR(300 MHz, acetone-d_6): δ 9.46 (s, 1H), 8.96 (d, J=1.48 Hz, 1H), 8.93 (s, 1H), 8.37–8.41 (m, 3H), 8.33 (d, J=1.97 Hz, 1H), 8.30 (d, J=2.67 Hz, 1H), 8.23 (d, J=8.91 Hz, 1H), 8.15(dd, J=7.66, 7.66 Hz, 1H), 7.37(s, 1H); ^{13}C NMR (75 MHz, acetone-d_6): δ 154.2, 134.2, 131.7, 131.1, 131.0, 129.9, 129.8, 128.2, 127.8, 127.0, 126.9, 126.8, 126.7, 126.6, 125.4, 125.0, 124.6, 122.2, 114.5, 113.4, 106.5. IR (KBr) 3442 (NH), 3314 (NH), 2242 (C≡N), 2198 (C≡N), 1603 (C=C, C=N), 1595 (C=C, C=N) cm^{-1}.

4.3. Metal ion binding study by UV–vis and fluorescence spectroscopy

Chemosensor **1** (25 μM) was added with different metal ions (100 μM). All spectra were measured in 1.0 mL acetonitrile–water solution (v/v=1/1, 10 mM HEPES buffer, pH 7.0). The light path length of cuvvet was 1.0 cm.

4.4. The pH dependence on Cu^{2+} binding in chemosensor 1 studied by fluorescence spectroscopy

Chemosensor **1** (25 μM) was added with Cu^{2+} (100 μM) in 1.0 mL acetonitrile–water solution (v/v=1/1, 10 mM buffer). The buffers were: pH 1–2, KCl–HCl; pH 2.5–4, KH_2PO_4–HCl; pH 4.5–6, KHP–NaOH; pH 6.5–10 HEPES.

4.5. Determination of the binding stoichiometry and the apparent association constants K_a of Cu(II) binding in chemosensor 1

The binding stoichiometry of **1**–Cu^{2+} complexes was determined by Job plot experiments.[16] The fluorescence intensity at 417 nm was plotted against molar fraction of **1** under a constant total concentration. The concentration of the complex approached a maximum intensity when the molar fraction was 0.5. These results indicate that chemosensor **1** forms a 1:1 complex with Cu^{2+}. The apparent association constants (K_a) of **1**–Cu^{2+} complexes were determined by the Benesi–Hildebrand Eq.1:[17, 18]

$$1/(F-F_0) = 1/\left\{K_a \times (F_{max}-F_0) \times \left[Cu^{2+}\right]\right\} + 1/(F_{max}-F_0) \quad (1)$$

where F is the fluorescence intensity at 417 nm at any given Cu^{2+} concentration, F_0 is the fluorescence intensity at 417 nm in the absence of Cu^{2+}, and F_{max} is the maxima fluorescence intensity at 417 nm in the presence of Cu^{2+} in solution. The association constant K_a was evaluated graphically by plotting $1/(F-F_0)$ against $1/[Cu^{2+}]$. Typical plots ($1/(F-F_0)$ vs $1/[Cu^{2+}]$) are shown in Fig. 6. Data were linearly fitted according to Eq. 1 and the K_a value was obtained from the slope and intercept of the line.

Acknowledgements

We gratefully acknowledge the financial supports of the National Science Council (ROC) and NationalChiao Tung University.

Supplementary data

^{1}H NMR and ^{13}C NMR spectra of Chemosensor **1**, EI-Mass and HRMS(EI) spectra of Chemosensor **1**, ^{1}H NMR spectra of Chemosensor **1** (5 mM) in the presence of different amount of Cu^{2+} in CD_3CN, IR spectra of Chemosensor **1** in the presence of Cu^{2+}. Supplementary data related to this article can be found online version at doi:10.1016/j.tet.2010.10.054.

References and notes

1. Frausto da Silva, J. J. R.; Williams, R. J. P. *The Biological Chemistry of Elements: The Inorganic Chemistry of Life*; Clarendon: Oxford, 1993; pp. 388–397.
2. Cowan, J. A. *Inorganic Biochemistry: An Introduction*; Wiley-VCH: New York, NY, 1997, pp 133–134.
3. Bull, P. C.; Thomas, G. R.; Rommens, J. M.; Forbes, J. R.; Cox, D. W. *Nat. Genet.* **1993**, *5*, 327–337.
4. Hahn, S. H.; Tanner, M. S.; Danke, D. M.; Gahl, W. A. *Biochem. Mol. Med.* **1995**, *54*, 142–145.
5. Barnham, K. J.; Masters, C. L.; Bush, A. I. *Nat. Rev. Drug Discovery* **2004**, *3*, 205–214.
6. Waggoner, D. J.; Bartnikas, T. B.; Gitlin, J. D. *Neurobiol. Dis.* **1999**, *6*, 221–230.
7. Vulpe, C.; Levinson, B.; Whitney, S.; Packman, S.; Gitschier, J. *Nat. Genet.* **1993**, *3*, 7–13.
8. Gonzales, A. P. S.; Firmino, M. A.; Nomura, C. S.; Rocha, F. R. P.; Oliveira, P. V.; Gaubeur, I. *Anal. Chim. Acta* **2009**, *636*, 198–204.
9. Becker, J. S.; Matusch, A.; Depboylu, C.; Dobrowolska, J.; Zoriy, M. V. *Anal. Chem.* **2007**, *79*, 6074–6080.
10. Liu, Y.; Liang, P.; Guo, L. *Talanta* **2005**, *68*, 25–30.
11. Ensafi, A. A.; Khayamian, T.; Benvidi, A. *Anal. Chim. Acta* **2006**, *561*, 225–232.
12. (a) Kaur, S.; Kumar, S. *Chem. Commun.* **2002**, 2840–2841; (b) Zheng, Y.; Gattas-Asfura, K. M.; Konka, V.; Leblanc, R. M. *Chem. Commun.* **2002**, 2350–2351; (c) Xu, Z.; Qian, X.; Cui, J. *Org. Lett.* **2005**, *7*, 3029–3032; (d) Royzen, M.; Dai, Z.; Canary, J. W. *J. Am. Chem. Soc.* **2005**, *127*, 1612–1613; (e) Zeng, L.; Miller, E. W.; Pralle, A.; Isacoff, E. Y.; Chang, C. J. *J. Am. Chem. Soc.* **2006**, *128*, 10–11; (f) Qi, X.; Jun, E. J.; Xu, L.; Kim, S.; Hong, J. S. J.; Yoon, Y. J.; Yoon, J. *J. Org. Chem.* **2006**, *71*, 2881–2884; (g) Xiang, Y.; Tong, A.; Jin, P.; Ju, Y. *Org. Lett.* **2006**, *8*, 2863–2866; (h) Yang, H.; Liu, Z.; Zhou, Z.; Shi, E.; Li, F.; Du, Y.; Yi, T.; Huang, C. *Tetrahedron Lett.* **2006**, *47*, 2911–2914; (i) Martinez, R.; Zapata, F.; Caballero, A.; Espinosa, A.; Tarraga, A.; Molina, P. *Org. Lett.* **2006**, *8*, 3235–3238; (j) Jun, E. J.; Won, H. N.; Kim, J. S.; Lee, K.-H.; Yoon, J. *Tetrahedron Lett.* **2006**, *47*, 4577–4580; (k) Zhang, X.; Shiraishi, Y.; Hirai, T. *Org. Lett.* **2007**, *9*, 5039–5042; (l) Li, G.; Xu, Z.; Chen, C.; Huang, Z. *Chem. Commun.* **2008**, 1774–1776; (m) Wu, S.; Liu, S. *Sens. Actuators, B* **2009**, *141*, 187–191; (n) Jung, H. S.; Kwon, P. S.; Lee, J. W.; Kim, J.; Hong, C. S.; Kim, J. W.; Yan, S.; Lee, J. Y.; Lee, J. W.; Joo, T.; Kim, S. *J. Am. Chem. Soc.* **2009**, *131*, 2008–2012; (o) Ballesteros, E.; Moreno, D.; Gomez, T.; Rodriguez, T.; Rojo, J.; Garcia-Valverde, M.; Torroba, T. *Org. Lett.* **2009**, *11*, 1269–1272; (p) Zhou, Y.; Wang, F.; Kim, Y.; Kim, S.; Yoon, J. *Org. Lett.* **2009**, *11*, 4442–4445; (q) He, G.; Zhao, X.; Zhang, X.; Fan, H.; Wu, S.; Li, H.; He, C.; Duan, C. *New J. Chem.* **2010**, *34*, 1055–1058; (r) Goswami, S.; Sen, D.; Das, N. K. *Org. Lett.* **2010**, *12*, 856–859; (s) Xu, Z.; Pan, J.; Spring, D. R.; Cui, J.; Yoon, J. *Tetrahedron* **2010**, *66*, 1678–1683.
13. Maeda, H.; Inoue, Y.; Ishida, H.; Mizuno, K. *Chem. Lett.* **2001**, 1224–1225.
14. Karpovich, D. S.; Blanchard, G. J. *J. Phys. Chem.* **1995**, *99*, 3951–3958.
15. (a) Lauher, J. W.; Ibers, J. A. *Inorg. Chem.* **1975**, *14*, 640–645; (b) MacLachlan, M. J.; Park, M. K.; Thompson, L. K. *Inorg. Chem.* **1996**, *35*, 5492–5499.
16. Senthilvelan, A.; Ho, I.; Chang, K.; Lee, G.; Liu, Y.; Chung, W. *Chem.—Eur. J.* **2009**, *15*, 6152–6160.
17. Benesi, H. A.; Hildebrand, J. H. *J. Am. Chem. Soc.* **1949**, *71*, 2703–2707.
18. Singh, R. B.; Mahanta, S.; Guchhait, N. *J. Mol. Struct.* **2010**, *963*, 92–97.